

Technique for measurement of fluorescence lifetime by use of stroboscopic excitation and continuous-wave detection

D. R. Matthews, H. D. Summers, K. Njoh, R. J. Errington, P. J. Smith, P. Barber, S. Ameer-Beg, and B. Vojnovic

A study of the practicality a simple technique for obtaining time-domain information that uses continuous wave detection of fluorescence is presented. We show that this technique has potential for use in assays for which a change in the lifetime of an indicator occurs in reaction to an analyte, in fluorescence resonance energy transfer, for example, and could be particularly important when one is carrying out such measurements in the scaled-down environment of a lab on a chip (biochip). A rate-equation model is presented that allows an objective analysis to be made of the relative importance of the key measurement parameters: optical saturation of the fluorophore and period of the excitation pulse. An experimental demonstration of the technique that uses a cuvette-based analysis of a carbocyanine dye and for which the excitation source is a 650 nm wavelength, self-pulsing AlGaInP laser diode is compared with the model. © 2006 Optical Society of America

OCIS codes: 140.5960, 170.2520, 170.3650, 300.2530.

1. Introduction

Using fluorescence to sense chemical or biochemical analytes has been demonstrated to be extremely useful for a wide range of applications. In some form fluorescence sensing is utilized in environmental monitoring, clinical chemistry, DNA sequencing and genetic analysis, cell identification in flow cytometry, and numerous imaging techniques. At the most basic level, a number of assays can be performed by simple monitoring of the reaction of the fluorescence intensity of a probe to an analyte. There are a number of disadvantages to this type of approach, including, but not limited to, issues with reliability, convenience, and ease of performing quantitative analyses, all of which can be overcome if the fluorescence lifetime is used as the indicator; the lifetime of a fluorophore is

independent of the system used to measure it¹ (provided that the appropriate convolution procedures are employed). Using the fluorescence lifetime as the indicator in an assay removes any ambiguities that arise in intensity-based measurements as a result of detector sensitivity, intensity of the excitation source, or indicator concentration. In addition the fluorescence lifetime gives information that would otherwise be averaged out in a steady-state measurement and can be particularly useful in resonance energy transfer measurements, for which the emission and absorption spectra of the species of interest overlap, or in collisional quenching assays.

Advances in microengineering have seen increasing interest in developing highly portable and even disposable lab-on-a-chip (or biochip) devices² for fluorescence sensing in point-of-care applications, and clearly it would be a major advantage to be able to perform lifetime sensing with such a device. Recent innovations have seen cell handling by electrophoresis,³ optical elements,⁴ microfluidic elements,⁵ and even excitation sources and detectors incorporated into such microscale systems.⁶ Devising a fully integrated system for fluorescence-lifetime sensing for which the excitation source (be it a laser diode or a LED) and the detector are included on the biochip, with the necessary high signal-to-noise ratio and time resolution required for a time-domain measurement, would be extremely challenging. At present the

D. R. Matthews (matthewsdr2@cf.ac.uk) and H. D. Summers are with the School of Physics and Astronomy, Cardiff University, 5 The Parade, Cardiff CF24 3YB, UK. K. Njoh, R. J. Errington, and P. J. Smith are with the School of Pathology, Cardiff University, Heath Park, Cardiff CF14 4XN, U.K. P. Barber, S. Ameer-Beg, and B. Vojnovic are with the Advanced Technology Development Group, Gray Cancer Institute, Mount Vernon Hospital, Northwood HA6 2JR, U.K.

Received 8 July 2005; revised 17 October 2005; accepted 22 October 2005.

0003-6935/06/092115-09\$15.00/0

© 2006 Optical Society of America

technique of choice for determining the lifetime of a fluorophore is time-correlated single-photon counting⁷ (TCSPC). Many other methods exist: detection by streak camera, upconversion techniques and stroboscopic gating, and optical boxcar methods (essentially the method now routinely used in lifetime imaging), but these have not been adopted on the scale of TCSPC. TCSPC is now the premier method because of its ability to determine decay lifetimes with high accuracy; each of the other methods is capable of this but is limited in another way. The instrumentation required for TCSPC is, in general, complex and expensive; systems often include mode-locked solid-state pump lasers such as the titanium sapphire laser, multichannel plate photomultiplier tube detectors, spectrometers, and electronics for processing the data collected by the detector. Whereas these issues are being addressed in terms of the availability of pulsed laser diodes and processing electronics (time-to-amplitude converter, constant fraction discriminator, etc.) in the form of personal computer plug-in boards, TCSPC and its associated components are not practical for a fully integrated portable lab-on-a-chip device.

Implementing lifetime measurements in a scaled-down environment in which detection and excitation would be integrated onto the biochip introduces an extra level of difficulty. The number of fluorescence photons generated would be extremely small (even in the event that a suitable laser could be integrated onto the chip for excitation) because of the greatly reduced sample size. In this type of environment we would expect collection efficiency to increase compared with that of a cuvette-based measurement, but even if such did occur, the on-chip detector would still need to be extremely sensitive to achieve the necessary single-photon counting. Avalanche photodiodes would be the ideal detectors because they can be fabricated on a micrometer scale, but there is still the problem of processing the signal, and this means either gating the avalanche photodiode or using a TCSPC-type system, all of which require high-specification electronics.

To overcome these difficulties we propose transferring the emphasis for time resolution from the detector to the excitation source. This can be achieved by employing a repetitively pulsed laser whose frequency of repetition can be varied such that either sufficient time elapses for the fluorophore to relax fully before reexcitation or the decay is restricted, eliciting an essentially dc response. As is described below, this technique potentially will permit the determination of fluorescence lifetimes in the nanosecond range in a completely dc-driven setup in which a time-averaged detector signal is generated in response to excitation pulses emitted by the laser source. More importantly, rather than as a competitor for existing time-domain detector measurements, we envisage this as a complementary technique for obtaining lifetime information from a fully integrated biochip environment in biological assays when differentiating between two fluorophore lifetimes is important.

The remainder of this paper is structured as follows: In Section 2 we describe the principles of the technique by means of an analysis that uses a set of three coupled first-order rate equations to identify and examine the important parameters when stroboscopic excitation is used. The practicalities of this measurement technique have been studied in detail, and Sections 3 and 4 are used to present the results of a comparative proof-of-principle investigation in which a self-pulsing AlGaInP laser diode is used to excite a carbocyanine fluorescent dye (Cy5) dissolved in either water or ethanol.

2. Principles of the Technique

The concept of stroboscopic excitation is based on the use of repetitive, fixed-intensity pulses with a variable period. It is the variation of the repetition frequency that provides temporal resolution. Within each period of the pulse train, equilibrium exists between the excitation energy absorbed and the energy emitted by the fluorophores. When the period of repetition of the excitation is much greater than the fluorescence lifetime, the fluorophore is allowed to relax fully before the arrival of the next pulse, and so maximum absorption is achieved. Conversely, at high repetition rates relaxation is restricted by the multiple-pulse train, and this reduces the excitation efficiency per pulse because part of the fluorophore population remains in an excited state. This leads to a time-integrated fluorescence intensity that is dependent on the ratio of the excitation pulse period to the fluorophore decay lifetime. A simple mathematical description of the fluorescence response can be obtained by tracking the number of fluorophores in the ground state, N_{gd} . If N_{ex} is the number of fluorophores in an excited state immediately following an excitation pulse, then the number in the ground state on arrival of the next pulse will be

$$N_{\text{gd}} = N - N_{\text{ex}} \exp\left(-\frac{T}{\tau}\right), \quad (1)$$

where N is the total number of fluorophores, T is the period of excitation, and τ is the decay lifetime of the fluorescence. The time-averaged fluorescence intensity, S , will be proportional to the frequency of the excitation source, f_{pulse} , and to the absorption efficiency, which is related to the ground-state fluorophore population. The following relation shows that the normal linear response in fluorescence intensity to increasing pulse frequency is altered to a saturated, nonlinear signal:

$$S \propto f_{\text{pulse}} \left[N - N_{\text{ex}} \exp\left(-\frac{T}{\tau}\right) \right]. \quad (2)$$

We stress that this is frequency-driven saturation rather than the intensity-driven saturation that is normally associated with a fluorophore population pumped to transparency. The decrease in signal, caused by reduced excitation efficiency, is controlled by

the two parameters, N_{ex} and T/τ . The ratio T/τ produces nonlinear behavior by limiting the relaxation of the excited population. N_{ex} acts as a scaling factor for the nonlinearity and is related to the degree of excitation of the system. At maximum absorbed power N_{ex} is equal to $N/2$ (transparency) and the degree of frequency-driven saturation is greatest. For low excitation power N_{ex} tends to zero and a linear response is maintained. Therefore in the implementation of this technique both the excitation power and the repetition frequency of the stroboscopic pulse source are important controlling parameters. It is important to note that although the accuracy of the technique is dependent on the degree of excitation it does not intrinsically require complete, intensity-driven saturation of the fluorophores, as we discuss below.

To study the stroboscopic technique in detail we numerically solve a set of rate equations that describe the excited fluorophore population and use the output from this model to provide a fit to the experimental data. This approach allows both the time-resolved and the time-averaged behavior of the system to be studied.

In general, most fluorescent dyes that are used in biological labeling applications are composed of large organic molecules, which have a myriad of rotational and vibrational energy states that reside within several molecular orbitals. It is the relative time scales of relaxation, subsequent to excitation by an optical source, throughout these many states that means the production of fluorescence photons can be dynamically modeled by use of a three-level rate-equation approximation. Absorption of photons typically occurs in several femtoseconds (in fact this will depend on the temporal profile of the excitation pulse), while vibrational relaxation and intersystem crossing characteristically take place on picosecond time scales, rates that are several orders of magnitude faster than the spontaneous production of fluorescence photons. This means that the presence of the vibrational and rotational states of the molecule can effectively be ignored. Fluorescence usually takes place between the first excited and ground singlet states, and, if the Stokes shift between absorption and excitation is to be accounted for, we require a three-level system. The optical processes that occurs within a collection of such three-level molecules can be described by the following simple, first-order differential equations:

$$\frac{dN_1}{dt} = -N_1 B_{13} W_{\text{ex}} + N_2 A, \quad (3)$$

$$\frac{dN_2}{dt} = N_3 V_{32} - N_2 A, \quad (4)$$

$$\frac{dN_3}{dt} = N_1 B_{13} W_{\text{ex}} - N_3 V_{32}. \quad (5)$$

Here N_1 represents the number of molecules residing in the ground singlet state and N_2 and N_3 are num-

bers ascribed to the portion of the population in the lower and upper vibrational levels, respectively, of the excited singlet state. B_{13} is the Einstein rate coefficient that describes stimulated absorption between the ground state and the upper vibrational level of the excited state. V_{32} is an effective rate that describes the rotational and vibrational relaxation. A is the rate coefficient for spontaneous production of photons, i.e., the rate of fluorescence decay, the inverse of which gives the fluorescence decay lifetime because nonradiative relaxation is ignored in the calculation (inclusion of a nonradiative component merely acts to scale the number of generated photons). The variable W_{ex} represents the intensity of the repetitive pulses used to excite the collection of molecules, and it is the effect of the amplitude (i.e., the number of excitation photons) and the frequency of W_{ex} that will be examined below. Each pulse in the train has a Gaussian line shape with a full width at half-maximum (FWHM) that is an input parameter for the model. Ideally the FWHM should tend to zero, but in reality an excitation laser is likely to produce pulses of finite width in the picosecond range. It should be noted that stimulated emission between the excited and ground states of the collection is negligible and has thus been omitted from the calculation. These equations were solved numerically subject to the constraint given by

$$N_1 + N_2 + N_3 = N. \quad (6)$$

The sum of the molecules in the ground and excited states is equivalent to the total number of molecules in the collection that is being modeled ($N = 100$). This numerical approach allows the molecular population and the number of generated photons to be time resolved such that the effects of pump intensity and optical saturation can be examined in detail. In what follows, the excitation intensity was quantified by the definition of a pumping ratio:

$$N_p = \frac{\text{Number of excitation photons per second}}{N}. \quad (7)$$

This gives the number of excitation photons per molecule in the collection, and the introduction of an extinction coefficient would merely scale this number.

The response of the fluorophore to interrogation by this type of pumping is demonstrated in Fig. 1, which shows the time-resolved response when the frequency of pulsation is increased. When the excitation pump intensity is low ($N_p = 1 \times 10^{-4}$) as in Fig. 1(a), each successive excitation pulse leads to a rise in the fluorescence signal. This is so because a small excited-state population is produced initially and therefore successive pulses increase the population until an equilibrium level is reached. The desired response of the fluorophores is shown in Fig. 1(b). Here the intensity of the exciting radiation is high

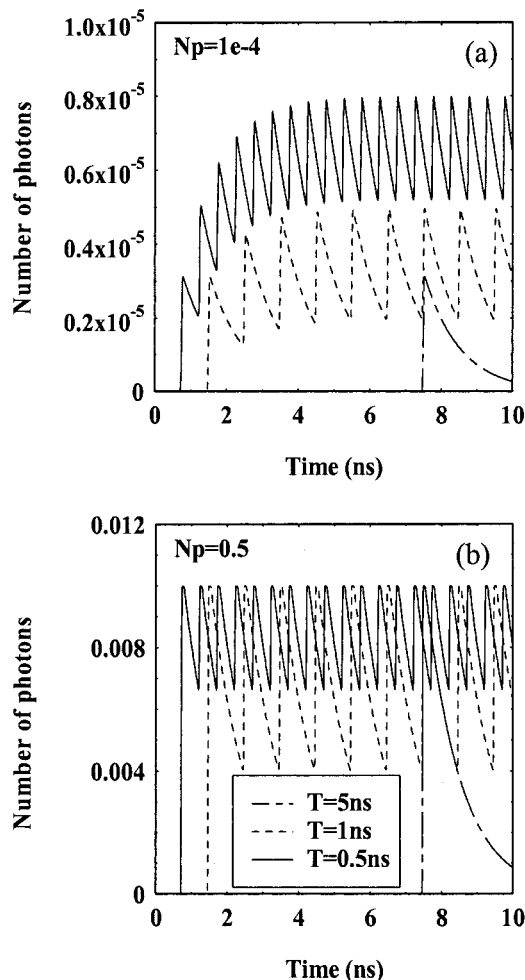


Fig. 1. Response of a collection of fluorescent molecules to multiple-pulse excitation with pumping ratios N_p of 1×10^{-4} and 0.5.

enough ($N_p = 0.5$) for the excited-state population to rapidly reach a dynamic equilibrium within each pump pulse cycle, and successive pulses then generate the same number of fluorescence photons.

As discussed above, the importance of this technique is that it will permit time-domain information to be obtained by use of cw detection. In this case it is the time-integrated signal that is obtained in a real measurement and, as expressions (1) and (2) show, a nonlinear response is produced when the pulse period is comparable to the lifetime of the fluorophore. By plotting the time-integrated intensity versus the ratio of the decay lifetime of the fluorophore to the excitation period (τ/T), as in Fig. 2, one can see the intrinsic behavior of this nonlinear response: The data for two different lifetime fluorophores match. When plotted in this fashion it is the level of optical pumping, or the excited-state population achieved, that determines whether the nonlinearity of the response can be resolved. For frequency-driven saturation to manifest itself a sufficient level of intensity-induced saturation must occur: A pumping ratio of

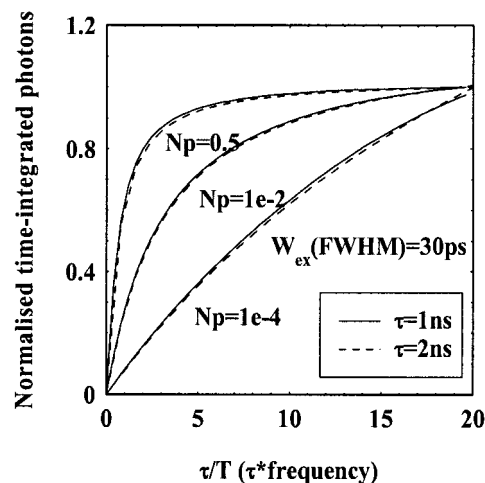


Fig. 2. Global behavior of time-integrated fluorescence generated under multiple-pulse excitation. Plotted in this manner, it is the intensity of the pump that determines the degree of nonlinearity in the data.

1×10^{-4} produces a linear response, whereas nonlinear behavior is apparent with $N_p = 0.5$.

The required level of intensity saturation for a nonlinear frequency response to become measurable is quantified in Fig. 3. This gives the ratio of time-integrated fluorescence emitted in response to pulse trains with repetition frequencies of 0.1 and 1 GHz; i.e., a linear response will provide a ratio of 10. This is plotted for a number of different decay lifetimes as a function of pumping level. A high-frequency limit of 1 GHz was chosen in this case because, as is described below, this is essentially the maximum frequency attainable from the self-pulsing laser used to verify the technique experimentally. At low pump intensity the time-integrated fluorescence tends to mimic any trend exhibited by W_{ex} because the molecular excited-state population is not saturated; i.e.,

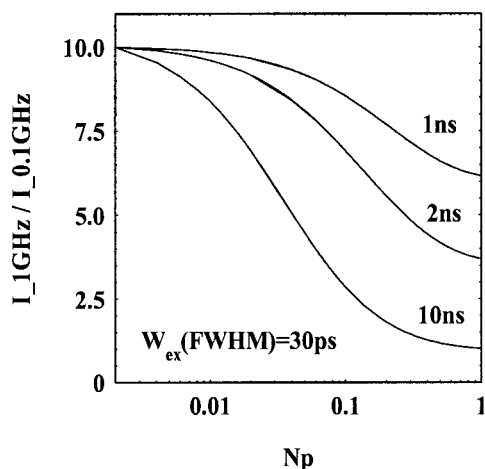


Fig. 3. Illustration of the intensity level of stroboscopic excitation necessary for a measurable frequency-driven nonlinearity to occur. Here the ratio of the time-integrated intensity generated by 1 and 0.1 GHz pulse trains plotted as a function of pumping level N_p .

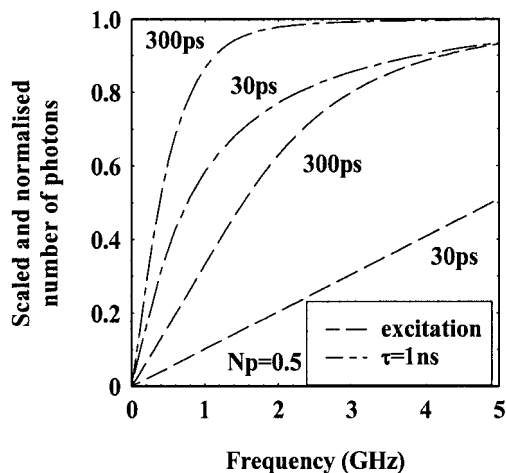


Fig. 4. Effect of excitation pulse width (FWHM) on the time-integrated number of photons generated during stroboscopic excitation. At 300 ps the excitation pulses do not return to zero, resulting in an element of cw pumping.

there is a linear increase in fluorescence in response to the linearly increasing excitation signal produced by sweeping the frequency of excitation. However, when the collection of molecules is pumped closer to saturation the time-integrated response becomes highly nonlinear with increasing frequency. Consider the data for the fluorophore with a 1 ns lifetime. In this case, with (τ/T) equal to a maximum value of 1, a nonlinear frequency response can be expected when the number of excitation photons per fluorophore is $\sim 10\%$. When the fluorophore's lifetime is increased to 10 ns (i.e., $\tau/T = 10$), the nonlinear effect can be observed with a pumping ratio as low as 1%.

As discussed in Section 3 below, the excitation pulses used to experimentally verify the technique were of the order of 300–400 ps, and so it is important to assess the effect of pulse width on a stroboscopic measurement. In Fig. 4 we compare the response of a 1 ns lifetime fluorophore to excitation pulses of 30 and 300 ps width. As the width of the pulses becomes comparable to the repetition period (as occurs at high frequency) the excitation intensity does not reach zero between successive pulses. As such, integration with respect to time of the excitation intensity yields a nonlinear pumping response as a function of frequency (as illustrated by the dashed curves in Fig. 4, which compares the time-integrated intensity when the excitation pulse width is 30 and 300 ps). This nonlinear response leads to an element of cw pumping and hence an exaggerated nonlinearity of the time-integrated fluorescence generated by the 300 ps excitation pulses.

3. Instrumentation

The rate-equation analysis given in Section 2 illustrates the simplicity of stroboscopic excitation to perform targeted, time-resolved assays with the inherent sensitivity that cw detection allows. Here we implement the technique by using a self-pulsing laser, operating at a wavelength of 650 nm, to excite

commercially available organic cyanine dye (Cy5), which emits in the deep red portion of the visible spectrum (emission peak at 670 nm). In this case the characteristics of the dye have been well matched to the laser performance (absorption peak and fluorescence lifetime in the nanosecond regime), as we seek to demonstrate the technique practically, establish likely accuracy, and explore the experimental boundaries within which it can be successfully applied. We therefore use a Hamamatsu streak camera to obtain fully time-resolved fluorescence in addition to time-averaged data. In this way we can objectively examine the optical saturation effects described in Section 2.

Self-pulsing semiconductor lasers are ideal sources for this technique, as they produce the stroboscopic pulse train by means of internal modulation and so are simple to use. The technique could be applied equally well to lasers for which external modulation is used to generate the excitation pulses. Self-pulsation is merely the phrase used to refer to the process by which the power output of laser diodes is self-modulated. This phenomenon is essentially a forced oscillation of the nonlinearly coupled electron and photon populations within the laser cavity. A source of saturable absorption is incorporated into the laser cavity, which introduces a feedback loop that results in a resonant bistability of the system. The period of the optical pulses generated is essentially the time required for establishing a population inversion within the laser cavity. This is directly related to the injection current (i.e., the rate of electron flow), and so one can control the period by varying the drive current applied to the laser.

The devices used in this study were typical Al-GaInP laser structures designed to emit light at a nominal wavelength of 650 nm, but, in addition to the standard laser design, they also include epitaxially grown saturable-absorber quantum wells. The full details of the layer structure can be found in Ref. 8–11.

Oxide-isolated stripe lasers, with widths that varied from 6 to 50 μm , were fabricated from the material; these were driven with a 25 ns (FWHM) current injection pulse at a repetition frequency of 20 kHz to reduce the effects of joule heating on the performance of the device and thus to help to maintain the regularity of the emitted pulse train. The lasers are not limited to a short drive pulse and in fact would continue to operate if the duration of the current injection pulse were to be extended considerably. However, the performance of these relatively wide-stripe devices degrades under such conditions, whereas narrowing the stripes results in a chirp in the pulsation frequency. These limitations are not intrinsic to the lasers and could be avoided by the use of advanced heat sinking technology, which would allow dc current drives to be used. Figure 5 shows the generation of optical pulses within the duration of the drive pulse for a 50 μm wide oxide stripe, 300 μm cavity-length device at several injection currents. Under these conditions, close to threshold, the laser produces a single 380 ps

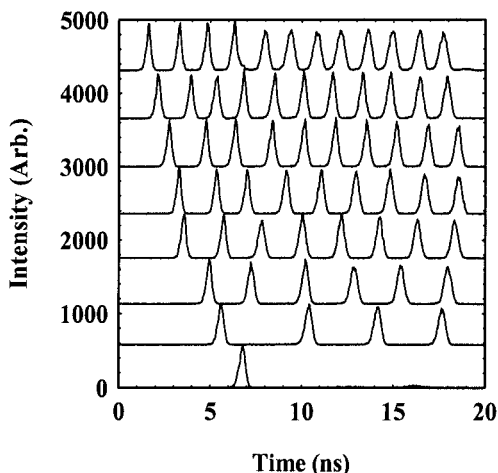


Fig. 5. Optical pulses obtained from a self-pulsing laser at several injection current levels.

(FWHM) wide Q -switched pulse. As the injection current level is increased further above threshold an increase in the number and frequency of the pulses is observed, with complete extinction of the stimulated emission between pulses for currents close to threshold. The lasers are capable of producing pulses up to a repetition frequency of 1.2 ± 0.2 GHz (the error of ± 0.2 GHz arises since the repetition frequency is determined by averaging over the whole duration of the pulse train and in fact there are variations in frequency at a particular injection current level). It is worth noting that under most operating conditions the laser produces pulses with a width in the range 300–400 ps (measured directly by streak camera detection) and we can therefore expect the pulse-width-related effects described in Section 2 when this type of laser is used to excite a fluorophore in a stroboscopic manner. There is also an experimental limitation of approximately 1.2 on the maximum τ/T ratio that we can reach, as the typical lifetime of Cy5 is approximately 1 ns. Thus the experiment lies in an area of parameter space (shown in Fig. 2 and 3) that produces a relatively weak nonlinear response.

4. Analysis

The response of Cy5 (dissolved in either water or ethanol) to stroboscopic excitation was measured in a standard orthogonal geometry with a 675 nm long pass filter to prevent scattered excitation light from entering the streak camera. As described above, under certain operating conditions the self-pulsing laser is capable of producing a single Q -switched pulse within the duration of the electrical injection pulse. When the laser is operated in this mode, it is an ideal source for standard time-domain measurements because the repetition rate is set by the current pulse generator used to drive the laser; which in this case is 20 kHz, which leaves ample time for the fluorophore to relax fully. A typical time-resolved decay curve for Cy5 dissolved in water is given in Fig. 6. The measurements were repeated for a number of concentra-

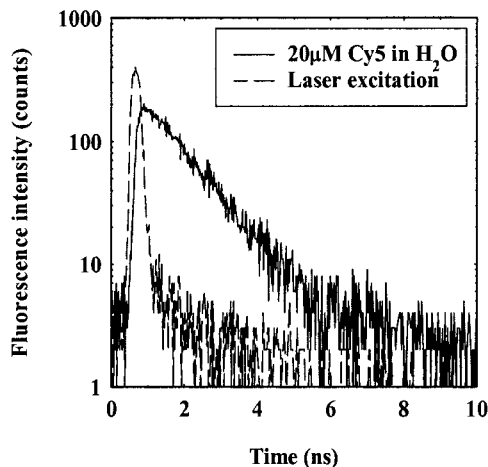


Fig. 6. Single-pulse excitation of Cy5 dissolved in water. The dashed curve shows the single Q -switched pulse generated by the laser under these operating conditions.

tions in water and ethanol and were characterized with monoexponential lifetimes; the quality of the fits was judged by use of the standard chi-square parameter. The data set is summarized in Table 1, which shows the lifetime of Cy5 to be 1.00 and 1.65 ns when the dye is dissolved in water and ethanol, respectively. These values show little variation with concentration and compare favorably with those published in the literature,¹² which gives the lifetime of Cy5 to be 0.91 ns in water and 1.32 ns in ethanol. The disparity in the ethanol data is attributed to a difference in purity of the distillations used.

Examples of excitation by multiple laser pulses at a number of frequencies are shown in Fig. 7 for 20 μ M solutions of Cy5 in ethanol and water. An unsaturated response is clear in the ethanol data, which show a trend similar to that displayed in Fig. 1(a). Each successive excitation pulse augments the excited-state population to produce an increasing level of fluorescence intensity. This becomes more apparent as the frequency of the excitation pulses is increased. The data for Cy5 dissolved in water, which has a higher effective excitation, show a response that is closer to intensity saturation. In this case the peak fluorescence generated by successive pulses is approximately constant.

Fluorescence generated by Cy5, such as that shown in Fig. 7, was time integrated over a fixed duration time window of 20 ns while the pulse repetition rate of the laser was varied to generate the data points given in Fig. 8 (the curves represent fits generated by

Table 1. Summary of Measured Fluorescence Lifetimes of Cy5 in Water and Ethanol

Solvent	Concentration (μ M)	τ (ns)	χ^2
H ₂ O	20	1.10	1.10
H ₂ O	100	0.95	1.19
EtOH	20	1.64	1.20
EtOH	100	1.61	1.10

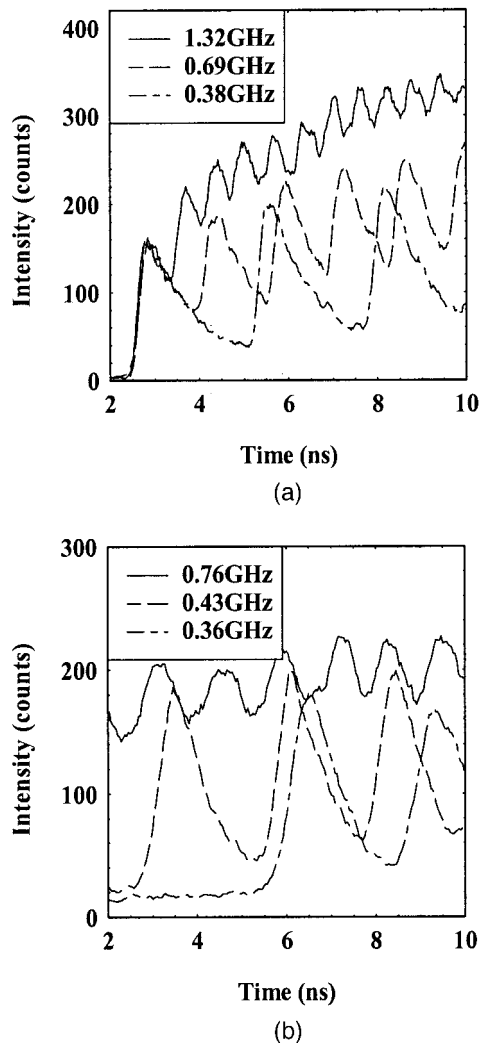


Fig. 7. Response to multiple-pulse excitation measured with a streak camera detector for Cy5 dissolved in (a) ethanol and (b) water. It is clear that in (b) the required level of intensity-driven saturation has been reached for the frequency-driven saturation to become apparent.

the rate-equation model with an excitation pulse width of 300 ps, which have been scaled to the time-integrated fluorescence intensity at the highest frequency reached in the experiment). These data show the expected frequency-driven nonlinear response, but an accurate extraction of the lifetime by use of the rate-equation model is difficult because the excitation level of the collection of fluorophores is unknown and the integration takes place over a limited number of pulse cycles. In general, the time-integrated data behave as expected from the time-resolved streak camera data, and broad agreement is seen with the predictions of the model. Figure 8(a) shows that the effective excitation of Cy5 in ethanol is so low that the frequency-driven nonlinearity cannot be seen and a determination of the lifetime is somewhat meaningless. The model provides some indication of the pumping ratio ($N_p \sim 0.02$), but the lifetime can take essentially any value in the model and still provide a

fit because the excited-state population, N_{ex} , is so small. As the time-resolved data of Fig. 7(b) showed, the solution of Cy5 in water was excited closer to saturation, and Fig. 8(b) illustrates that in this case a nonlinear response is clearly seen. Single-pulse excitation showed the lifetime of Cy5 in water to be 1 ns. This value was taken as an initial fit in the model to estimate a value for N_p . A range of fits with various lifetimes was then generated. A fit to the experimental data is obtained within a range of 1–1.5 ns. Of course, one could use N_p as a second free parameter to obtain a value for τ : As N_p is decreased, the value of lifetime must then necessarily increase to produce a fit to the data.

Although the error margin in the measurement presented seems large when it is compared with those for more traditional time-domain measurements, as mentioned in Section 1 we can see this technique as useful in targeted assays for which a significant lifetime change of the fluorophore occurs as a result of interaction with an analyte. In this type of assay *a priori* information, obtained by use of more-traditional time-domain techniques, about the change in lifetime that occurs owing to, for example, an alteration of the local environment or energy transfer in the presence of the analyte would be used in congruence with the stroboscopic technique: In essence this information would be a calibration. The assay of interest is then one concerned with detecting any changes in lifetime experienced by the fluorescent label rather than with determining an absolute lifetime.

The significance of these experimental data for this type of differential assay can be explained with reference to Figs. 2 and 3. A maximum value of $\tau/T \approx 1$ is achieved in the experiment, but this can be increased by the use of alternative, long-lifetime probes or the development of higher-frequency lasers. Figure 8(b) shows a comparison of the Cy5 data with a modeled response for a fluorescent species that has a 10 ns lifetime (CdSe colloidal nanocrystals, for example^{13,14}), increasing the τ/T maximum to 10. It is obvious that the degree of frequency-induced nonlinearity is much more pronounced in this case and would make determination of a decay lifetime simpler, but more importantly, this order of magnitude increase in τ/T amply illustrates the level of contrast that can be achieved in an assay in which a change in lifetime occurs. Figure 3 shows how this contrast varies with the intensity of the pump (N_p). At the level of pumping seemingly achieved in the experiment, the magnitude of the contrast between lifetimes of 1 and 2 ns is small. This means that, with the current level of error, it would be difficult to distinguish this transformation of lifetime. However, the technique, in its current state of development, would be adequate to perform an assay where there is a reduction in lifetime from 10 to 1 ns. This kind of lifetime response has been achieved in fluorescence resonant energy transfer based assays, where, as a result of near-field dipole interaction, two fluorescent probes (they need not both be fluorescent as long as the emission of the donor overlaps the absorption of the acceptor), be

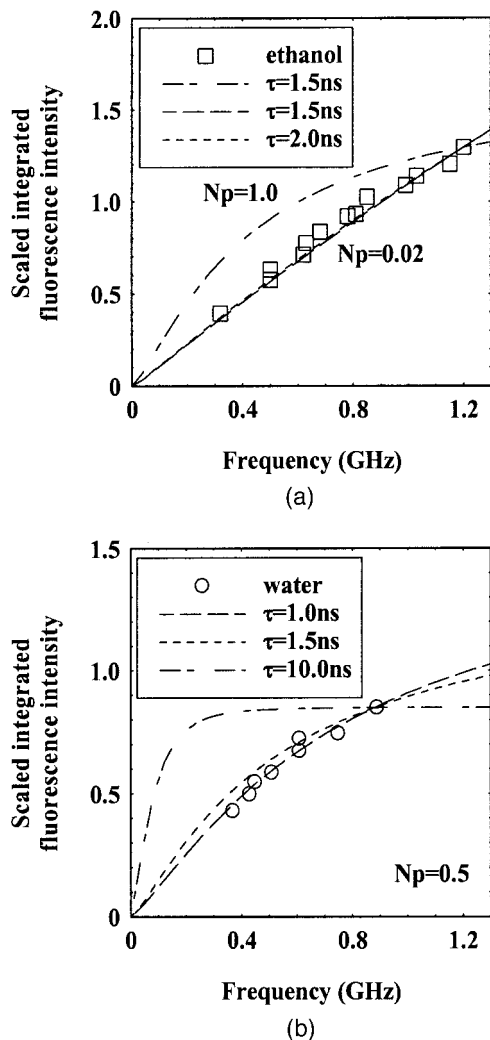


Fig. 8. Time-integrated fluorescence intensity obtained from a streak camera and plotted as a function of self-pulsation frequency for Cy5 dissolved in ethanol and in water.

they organic dyes or semiconductor nanocrystals, can exchange energy, causing a change in the decay lifetime of one or both of the donor and acceptor species. An assay, for example, may be one in which a fluorescent species binds to DNA or a protein of interest, fluorescence resonant energy transfer processes occur, and the change in lifetime of the fluorophore is detected. Clearly, in a biochip environment this could be done as a single-cell-based analysis but, as discussed above, would be extremely difficult, if not impossible, to do with traditional time-domain-based techniques. The simplicity of the stroboscopic technique and the fact that it makes use of inherently sensitive detection makes it an excellent candidate for such biochip-based differential assays.

5. Summary

We have presented simulated and experimental data showing that stroboscopic excitation is a useful method for retrieving time-domain information by using a cw detector. A rate-equation model was used to demonstrate the principles of the measurement

technique with particular attention paid to the effects of intensity-induced saturation of the excited fluorophore population. The technique was shown to work in a real measurement for which a self-pulsing 650 nm wavelength laser diode was used to excite a commercially available fluorescent dye. This permitted a full, objective examination of the important parameters for implementing the technique. It was shown by an intrinsic analysis that to obtain an accurate lifetime from the measurement it is necessary for $\tau/T > 1$. If this is achieved, then the fluorescence lifetime can be determined at excitation intensities well below that required for complete saturation of the signal. The technique is seen as particularly useful in microscaled assays suitable for lab-on-a-chip applications for which high-sensitivity cw detectors could be used to detect the change in the lifetime of a fluorescent species that would be indicative of resonance energy transfer, a chemical reaction, or collisional quenching.

This study was funded under the UK Research Councils' Basic Technology Program as part of the Optical Biochips Project.

References

1. J. R. Lakowicz, *Principles of Fluorescence Spectroscopy*, 2nd ed. (Kluwer Academic/Plenum, 1999).
2. C. H. Ahn, J.-W. Choi, G. Beaucage, J. H. Nevin, J.-B. Lee, A. Puntambekar, and J. Y. Lee, "Disposable smart lab on a chip for point-of-care clinical diagnostics," *Proc. IEEE* **92**, 154–173 (2004).
3. R. Pethig, J. P. H. Burt, A. Parton, N. Rizvi, M. S. Talary, and J. A. Tame, "Development of biofactory-on-a-chip technology using excimer laser micromachining," *J. Micromech. Microeng.* **8**, 57–63 (1998).
4. J. C. Roulet, R. Volkel, H. P. Herzig, E. Verpoorte, N. F. de Rooij, and R. Dandliker, "Performance of an integrated microoptical system for fluorescence detection in microfluidic systems," *Anal. Chem.* **74**, 3400–3407 (2002).
5. B. H. Weigl, R. L. Bardell, and C. R. Cabrera, "Lab-on-a-chip for drug development," *Adv. Drug Deliv. Rev.* **55**, 349–377 (2003).
6. E. Thrush, O. Levi, W. Ha, G. Carey, L. J. Cook, J. Deich, S. J. Smith, W. E. Moerner, and J. S. Harris, "Integrated semiconductor vertical-cavity surface-emitting lasers and PIN photodetectors for biomedical fluorescence sensing," *IEEE J. Quantum Electron.* **40**, 491–498 (2004).
7. D. V. O'Connor and D. Phillips, *Time-Correlated Single Photon Counting* (Academic, 1984).
8. H. D. Summers and P. Rees, "Thermal limitation of self-pulsation in 650 nm AlGaInP laser diodes with an epitaxially integrated absorber," *Appl. Phys. Lett.* **71**, 2665–2667 (1997).
9. H. D. Summers and P. Rees, "High-temperature operation of 650-nm wavelength AlGaInP self-pulsating laser diodes," *IEEE Photon. Technol. Lett.* **10**, 1217–1219 (1998).
10. D. R. Jones, P. Rees, I. Pierce, and H. D. Summers, "Theoretical optimization of self-pulsating 650-nm-wavelength AlGaInP laser diodes," *IEEE J. Sel. Top. Quantum Electron.* **5**, 740–744 (1999).
11. H. D. Summers, C. H. Molloy, P. M. Smowton, P. Rees, I. Pierce, and D. R. Jones, "Experimental analysis of self-pulsation in 650-nm-wavelength AlGaInP laser diodes with epitaxial absorbing layers," *IEEE J. Sel. Top. Quantum Electron.* **5**, 745–749 (1999).
12. V. Buschmann, K. D. Weston, and M. Sauer, "Spectroscopic

- study and evaluation of red-absorbing fluorescent dyes," *Bioconjugate Chem.* **14**, 195–204 (2003).
13. G. Schlegel, J. Bohnenberger, I. Potapova, and A. Mews, "Fluorescence decay time of single semiconductor nanocrystals," *Phys. Rev. Lett.* **88**, 137401 (2002).
 14. I. Chung and M. G. Bawendi, "Relationship between single quantum-dot intermittency and fluorescence intensity decays from collections of dots," *Phys. Rev. B* **70**, 165304 (2004).
 15. P. Alivisatos, "The use of nanocrystals in biological detection," *Nature Biotechnol.* **22**, 47–52 (2004).